Strehl-constrained reconstruction of post-adaptive optics data & the Software Package AIRY, v. 6.1

Marcel Carbillet[a], Andrea La Camera[b], Jérémy Deguignet[a,c], Marco Prato[d], Mario Bertero[b], Éric Aristidi[a], Patrizia Boccacci[b]

[a]UMR 7293 J.-L. Lagrange, Université de Nice Sophia-Antipolis/CNRS/Observatoire de la Côte d'Azur, Parc Valrose, 06100 Nice, France;
[b]Dipartimento di Informatica, Bioingegneria, Robotica e Ingegneria dei Sistemi (DIBRIS), Università di Genova, Via Dodecaneso 35, 16145 Genova, Italy;
[c]Master Imagerie et Modélisation Astrophysique et Géophysique, Espace et Environnement (IMAG2E), Université de Nice Sophia-Antipolis, Parc Valrose, 06100 Nice, France;
[d]Dipartimento di Scienze Fisiche, Informatiche e Matematiche, Università di Modena e Reggio Emilia, via Campi 213/b, 41125 Modena, Italy.

ABSTRACT

We first briefly present the last version of the `Software Package AIRY`, version 6.1, a `CAOS`-based tool which includes various deconvolution methods, accelerations, regularizations, super-resolution, boundary effects reduction, point-spread function extraction/extrapolation, stopping rules, and constraints in the case of iterative blind deconvolution (IBD). Then, we focus on a new formulation of our Strehl-constrained IBD, here quantitatively compared to the original formulation for simulated near-infrared data of an 8-m class telescope equipped with adaptive optics (AO), showing their equivalence. Next, we extend the application of the original method to the visible domain with simulated data of an AO-equipped 1.5-m telescope, testing also the robustness of the method with respect to the Strehl ratio estimation.

Keywords: post-AO imaging, iterative blind deconvolution, Strehl constraint, `Software Package AIRY`, `CAOS Problem Solving Environment`.

1. OUTLINE

The goal of this paper is twofold. First, we briefly present the last version of the `Software Package AIRY`, an `IDL`-written `CAOS`-based numerical tool the main aim of which is the simulation and, overall, the deconvolution of post-AO data. It includes various methods which are detailed in Section 2.

The second goal of this paper is to present the last results concerning the development of one of the deconvolution methods included in the `Software Package AIRY`: an iterative blind deconvolution (IBD) method with the application of a constraint on the data Strehl ratio (SR). Section 3 presents hence the two versions of our Strehl-constrained (SC) IBD algorithm, a comparison between their performance, showing their practical equivalence, and a study about the robustness of the method with respect to the actual SR evaluation. These studies are based on numerical simulations of an 8-m class AO-equipped telescope delivering near-infrared images, and of a 1.5-m class AO-equipped telescope for the visible domain. Finally, Sec. 4 presents our conclusions and perspectives for this on-going research work.

Further author information: (Send correspondence to M.C./A.L.C.)
M.C.: E-mail: marcel.carbillet@unice.fr, Telephone: +33 492076328
A.L.C.: E-mail: andrea.lacamera@unige.it, Telephone: +39 010 353 6609

Adaptive Optics Systems IV, edited by Enrico Marchetti, Laird M. Close, Jean-Pierre Véran, Proc. of SPIE Vol. 9148, 91484U · © 2014 SPIE
CCC code: 0277-786X/14/$18 · doi: 10.1117/12.2058525

2. THE SOFTWARE PACKAGE AIRY, VERSION 6.1

The `Software Package AIRY`[1,2] is a software tool designed to perform the simulation and/or deconvolution of astronomical images, a priori post-adaptive optics (AO) ones, and coming from monolithic or even binocular telescopes. It is written in `IDL` and it is part of the `CAOS Problem Solving Environment` (`CAOS PSE`)[3,4]. The `Software Package AIRY`, v. 6.1, summarizes fourteen years of developments and includes various deconvolution methods (Richardson-Lucy (RL or LR), Ordered Subset Expectation Maximization (OSEM), Image Space Reconstruction Algorithm (ISRA), OS-ISRA, Scaled Gradient Projection (SGP)), accelerations (Biggs & Andrews), regularizations (Tikhonov, Laplacian, entropy, edge-preserving, high-dynamic range), special methods (super-resolution, boundary effects reduction, point-spread function (PSF) extraction/extrapolation), stopping rules, iterative blind deconvolution (IBD), including constraints on the Strehl ratio (SR) and on the bandpass). The main latest enhancements concerning this version 6.1 are the implementation of the SGP method and a new formulation of our method of Strehl-constrained (SC) IBD. Let us now detail the points listed below in the following subsections.

2.1 General introduction

The imaging model used as a basis of the deconvolution algorithms implemented in the `Software Package AIRY` is that proposed by Snyder et al. (1993)[5]; if we assume to have p detected images $\mathbf{g}_j$, with $j = 1, \ldots, p$ (globally denoted as $\mathbf{g}$), of the unknown scientific object $\mathbf{f}$, all detected by means of a CCD camera, then for each image we have:

$$\mathbf{g}_j(\mathbf{m}) = \mathbf{g}_j^{(\mathrm{obj})}(\mathbf{m}) + \mathbf{g}_j^{(\mathrm{back})}(\mathbf{m}) + \mathbf{g}_j^{(\mathrm{ron})}(\mathbf{m}) \ , \tag{1}$$

where $\mathbf{g}_j^{(\mathrm{obj})}(\mathbf{m})$ is the number of photo-electrons arising from the object radiation; $\mathbf{g}_j^{(\mathrm{back})}(\mathbf{m})$ is the number of background photo-electrons (including sky background, dark current, and bias) and $\mathbf{g}_j^{(\mathrm{ron})}(\mathbf{m})$ is the amplifier read-out noise (RON). The first two terms are described by a Poisson process, the first with expected value $(\mathbf{A}_j\mathbf{f})(\mathbf{m})$ and the latter with expected value $\mathbf{b}_j(\mathbf{m})$. The last term is described by an additive Gaussian process, with expected value μ and variance σ^2. Without changing the statistics, we assume μ=0 for simplicity. Moreover, as shown by Snyder et al. (1995)[6], it is possible to treat the RON as a Poisson process if its variance σ^2 is added to the detected image (and, therefore, also to its expected value). In conclusion the detected images can be treated as realizations of Poisson processes, thanks to the statistical independence of the three terms in Eq. (1).

As concerns the matrix $\mathbf{A}_j$, appearing in the expected value of the object radiation and describing the effect of the optical components and the atmosphere, we assume that it can be described by a space-invariant PSF, so that, by indicating with $\mathbf{K}_j$ the j-th PSF normalized to unit volume ($\sum_{n \in R} \mathbf{K}_j(\mathbf{n}) = 1$), we can write:

$$(\mathbf{A}_j\mathbf{f})(\mathbf{m}) = \sum_{\mathbf{n} \in R} \mathbf{K}_j(\mathbf{m} - \mathbf{n})\mathbf{f}(\mathbf{n}) \ , \quad \mathbf{m} \in S \ , \tag{2}$$

where, for generality, we have assumed that the image and object domains do not necessarily coincide (this case is considered in the approach used for boundary effect correction).

In a maximum likelihood approach with data satisfying the assumption of Poisson statistics, according to the seminal paper of Shepp & Vardi (1982)[7] (see also Bertero et al., 2009[8]), the deconvolution methods consists in the minimization, with the additional constraint of non-negativity $\mathbf{f} \geq 0$, of a generalized Kullback-Leibler (KL) divergence given by:

$$J_0(\mathbf{f}; \mathbf{g}) = \sum_{j=1}^{p} \sum_{\mathbf{m} \in S} \left\{ \mathbf{g}_j(\mathbf{m}) \log \frac{\mathbf{g}_j(\mathbf{m})}{(\mathbf{A}_j\mathbf{f} + \mathbf{b}_j)(\mathbf{m})} + (\mathbf{A}_j\mathbf{f} + \mathbf{b}_j)(\mathbf{m}) - \mathbf{g}_j(\mathbf{m}) \right\} \ ; \tag{3}$$

this functional measures the discrepancy between the computed images associated to $\mathbf{f}$ and the detected images $\mathbf{g}$ and can be called *data-fidelity function*. In this equation images and backgrounds are modified in order to take into account the RON contribution, as indicated above.

The minimizers of J_0 do not provide a reliable solution of the reconstruction problem except in the case of stellar fields (Bertero et al., 2009 [8]). In the case of complex scientific targets it may be convenient to introduce a suitable prior, expressing known properties of the solution, in the framework of a Bayesian approach, as proposed in Geman & Geman (1984)[9]. In such a case, if we denote as $J_R(\mathbf{f})$ the negative logarithm of the prior, then the functional to be minimized takes the following form:

$$J_\mu(\mathbf{f};\mathbf{g}) = J_0(\mathbf{f};\mathbf{g}) + \mu J_R(\mathbf{f}) \ . \tag{4}$$

The functional $J_R(\mathbf{f})$ can be called *regularization function* and the parameter $\mu > 0$ can be called *regularization parameter*.

2.2 Deconvolution methods

In this subsection we briefly describe the deconvolution methods implemented in the `Software Package AIRY`. For a reference we give the RL[10, 11] algorithm which we write in the following form:

$$\mathbf{f}^{(k+1)} = \mathbf{f}^{(k)}\mathbf{C}^{(k)}(\mathbf{g}) \quad , \quad \mathbf{C}^{(k)}(\mathbf{g}) = \mathbf{A}^T \frac{\mathbf{g}}{\mathbf{A}\mathbf{f}^{(k)} + \mathbf{b}} \ ; \tag{5}$$

$\mathbf{C}^{(k)}(\mathbf{g})$ will be called the correction factor. Then the implemented methods for (possibly multiple) image deconvolution are the following.

- **Multiple Image Richardson Lucy (MRL)** - The algorithm is obtained from Eq. (5) by replacing the correction factor with the sum of the correction factors associate with the p detected images[12];
- **Ordered Subsets Expectation maximization (OSEM)** - Each iteration consists in a cycle over the p images, taken in a given order, each step of the cycle consisting of an RL iteration with the correction factor corresponding to the image associated with the step[12, 13].
- **Biggs-Andrews (BA) acceleration method** - It is the method proposed by Biggs & Andrews (1998)[14], which consists in extrapolating the reconstructions of the scientific object obtained from the outputs of two previous iterations and in applying the next iteration (of RL or MRL or OSEM) to the result of the extrapolation process.
- **Scaled Gradient Projection (SGP) method** - This method, proposed by Bonettini et al. (2009)[15] is inspired by the fact that the RL (or MRL) method is a scaled gradient method for the minimization of the functional of Eq. (3). It is a very efficient method. Its implementation for astronomical images is described in Prato et al. (2012)[16], where it is shown that it can be faster than OSEM and sometimes also faster than the BA method applied to RLM.
- **Split-Gradient Method (SGM)** - This method, proposed by Lantéri et al. (2002)[17] is a method which provides a generalization of RL to the case of regularization, i.e. minimization of the functional of Eq. (4). It can be extended both to the case of MRL and to the case of OSEM. These extensions are implemented in the `Software Package AIRY`. Work is in progress for extending the approach also to SGP. It has been implemented for functions $J_R(\mathbf{f})$ corresponding to the following regularizations:
  1. Tikhonov regularization in terms of the ℓ_2 norm of the object or of its discrete Laplacian[17];
  2. maximum entropy regularization in terms of the entropy of the object relative to a reference object, for instance a constant array[17];
  3. edge-preserving regularization[18, 19];
  4. high-dynamic range regularization, applicable in the case of disjoint objects with very different intensities (Anconelli et al., 2006a[20]).

- **Boundary effect correction** - For all the deconvolution methods one can also choose a version for boundary effect correction. This is based on an approach proposed by Bertero & Boccacci (2005)[21] in the case of single image and by Anconelli et al. (2006b)[22] in the case of multiple images. The main idea is to reconstruct the object on an array R broader than the array S of the detected image after extension of the image from S to R by zero padding.

2.3 Stopping rules

All the algorithms enumerated in the previous section are iterative so that they must be stopped. This is a crucial point because different algorithms have different behaviour. For instance MRL, OSEM, BA and SGP can be pushed to convergence in the case of the reconstruction of a stellar field while, in the case of a diffuse object such as a nebula or a distant galaxy they must be stopped before convergence. Indeed, in these cases, they show the so-called *semi-convergence* behaviour: the iterations first approach a sensible solution and then they go away. On the other hand, in the case of SGM or of other iterative algorithm for regularized solutions, the iterations must be pushed to convergence, independently of the value of μ. In such a case the difficult problem is the choice of a sensible value of μ.

As a consequence of the previous remarks the following stopping rules can be selected for the iterative algorithms implemented in the `Software Package AIRY`:

- total number of iterations, decided by the user;
- number of iterations for pushing the algorithm to convergence, which is decided on the behaviour of the objective function: given a tolerance τ, selected by the user, stop the algorithm at the iteration k such that:
$$|J(\mathbf{f}^{(k)};\mathbf{g}) - J(\mathbf{f}^{(k-1)};\mathbf{g})| \leq \tau J(\mathbf{f}^{(k-1)};\mathbf{g}) \ , \tag{6}$$
the objective function J being J_0 or J_μ, depending on the application;
- in the case of simulated data, the algorithms MRL, OSEM, BA and SGP can be stopped when the reconstruction error, defined as the relative rms error between the iterate and the ground-truth, has a minimum (semi-convergence criterion);
- in the case of real data one can use, for stopping the iterations, a discrepancy principle as that described in Bertero et al. (2011)[23].

In all cases a maximum number of iterations must be provided by the user.

2.4 Special methods

In this subsection we describe other methods contained into the `Software Package AIRY` that are directly related to deconvolution.

- **Super-resolution** - It is known that methods such as RL, OSEM and SGP, have a moderate super-resolution effect; nevertheless, by a suitable initialization of the algorithm it is possible to increase this effect. We suppose that the object has an angular size close to the angular resolution of the instrument; in this case we can improve the resolution by restricting the reconstruction to this domain[24]. To do that, we first define a mask as a function which is equal to one in the super-resolution domain and zero elsewhere, and we then note that each algorithm described in section 2.2 can be seen as a particular case of a general scaled gradient method:
$$\mathbf{f}^{(k+1)} = \mathbf{f}^{(k)} + \lambda_k \left(\mathcal{P}_+(\mathbf{f}^{(k)} - \alpha_k D_k \nabla J(\mathbf{f}^{(k)};\mathbf{g})) - \mathbf{f}^{(k)} \right) . \tag{7}$$
In the case of RL and OSEM, the projection $\mathcal{P}_+$ on the non-negative pixels can be avoided if the starting point of the algorithm is multiplied by the mask of the domain (the pixels with zero values will not change in

all iterations). On the contrary, in the case of SGP, the mask must be multiplied at each iteration at the end of the projection step. A considerable improvement of resolution can be obtained in this way. A discussion of the method as well as of a possible oversampling by means of data re-binning is discussed in Anconelli et al. (2005)[25]. The module `DEC` of the `Sofware Package AIRY` permits to perform reconstructions with super-resolution, and the super-resolution method is explained in two example projects provided with the package.

- **PSF extraction and extrapolation -** In the case of ground-based telescopes equipped with AO systems the PSF is not always known with sufficient precision. In case of stellar images, when different stars are present in the field-of-view of the instrument, the PSF can be extracted from the input image. Very often the image of the star is quite small (few tens of pixels) and it is smaller than the full image. Of course it could be extended by zero-padding, but this extension may not be suitable for image deconvolution. For this reason we implemented an extrapolation of the PSF outside the extraction domain by means of a suitable Moffat function, with the form:

$$M(r) = \frac{a}{(b + r^2)^{\beta}} \quad , \tag{8}$$

  where r is the distance from the centre (the star), a and b are parameters to be fitted and β is the exponent of the Moffat function. The procedure is described in La Camera et al. (2007)[26] and is implemented within module `PEX` of the `Software Package AIRY`.

3. THE STREHL-CONSTRAINED ITERATIVE BLIND DECONVOLUTION

3.1 Original vs. new formulation

The original SCIBD algorithm, proposed in Desiderà & Carbillet (2009)[27], consists in constraining the SR of the reconstructed PSF, by slightly blurring the latter at the exit of the PSF reconstruction box and at each global iteration of the algorithm (see block diagram within Fig. 1), with a small Gaussian untill its SR lowers down to the estimated data SR.

The new formulation, proposed in Prato et al. (2013)[28], includes the Strehl constraint within the PSF box by substituting the RL algorithm with SGP, whose iterates automatically satisfy all the constraints (SR, non-negativity and normalization) thanks to the projection performed within the descent direction. The same substitution is also performed in the image box, imposing non-negativity and flux conservation within the inner SGP iterations themselves. The presence of an adaptive steplength parameter could also allow to speed-up the convergence of the algorithm.

We first consider here the same case study as for the original paper[27], i.e. the one "eye" of the 8-m class telescope LBT equipped with the AO system FLAO, and working in band H. An expansion of the original test range of SR towards lower values (down to 0.06) has also been performed. We find a rather good agreement between the two approaches for both the PSF reconstruction and the object reconstruction (see Fig. 2).

3.2 Towards visible wavelengths

Figure 3 shows another test on binary star data simulated by means of the `Software Package CAOS`[29] again, but here for the case-study of the 1.52-m telescope MéO (plateau de Calern, France), equipped with the AO system ODISSEE (developped by ONERA and recently installed at MéO), in the visible domain (R band), with SR of 0.31, 0.21, 0.11, and 0.04. First row is for the raw images, second row for the reconstructed objects with IBD, third row for the reconstructed objects with SCIBD, and, for sake of comparison with a somehow ideal deconvolution case, last row is for the reconstructed objects with an inverse-crime RL (PSF perfectly known).

Left part of Fig. 4 shows a quantitative comparison of the four methods considered (aperture photometry from the raw images, the standard IBD reconstructions, the SCIBD reconstructions, and the inverse-crime RL reconstructions). It clearly shows that, first of all, deconvolution is usefull not only in order to well define the exact morphology of the object and its relative astrometry (clearly seen from Fig. 3), but also for the relative photometry, performing always better in that sense than when simply considering the raw images. Second, it

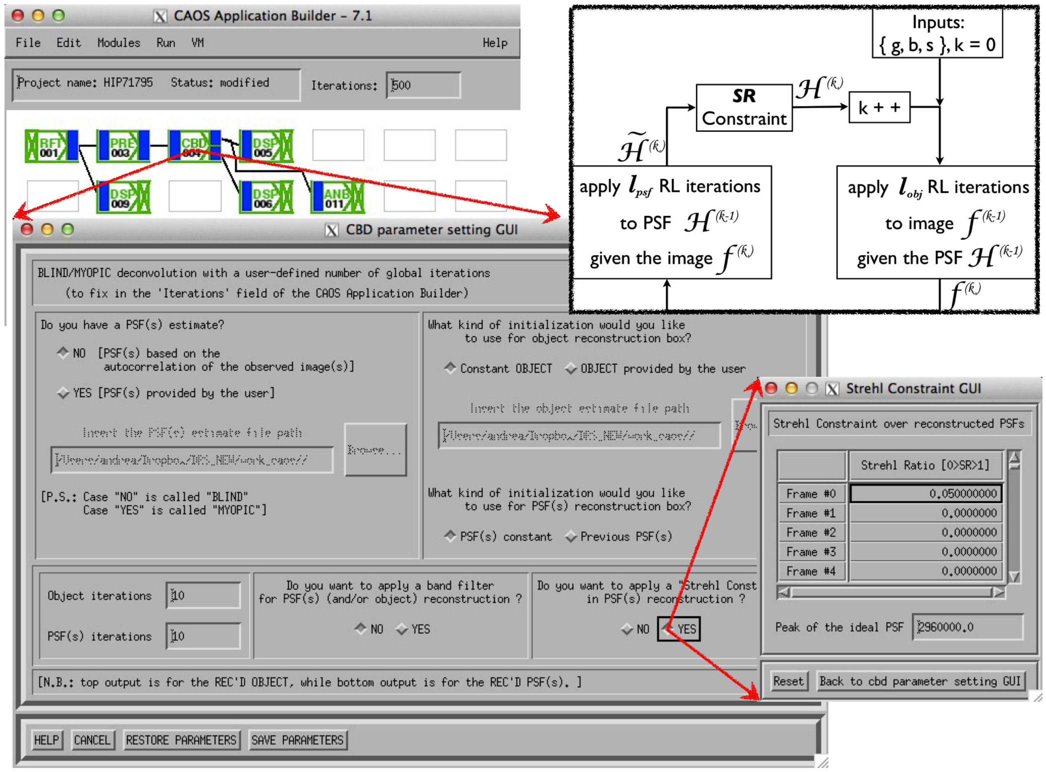

Figure 1. “Project” of Strehl-constrained IBD implemented within the `CAOS Application Builder` (the global user interface of the `CAOS PSE`, top-left part of the figure). The GUI of module `CBD` (for Constrained Blind Deconvolution) is shown open, with the sub-GUI corresponding to the Strehl constraint option. Top-right part also shows the block diagram of the SCIBD original formulation.

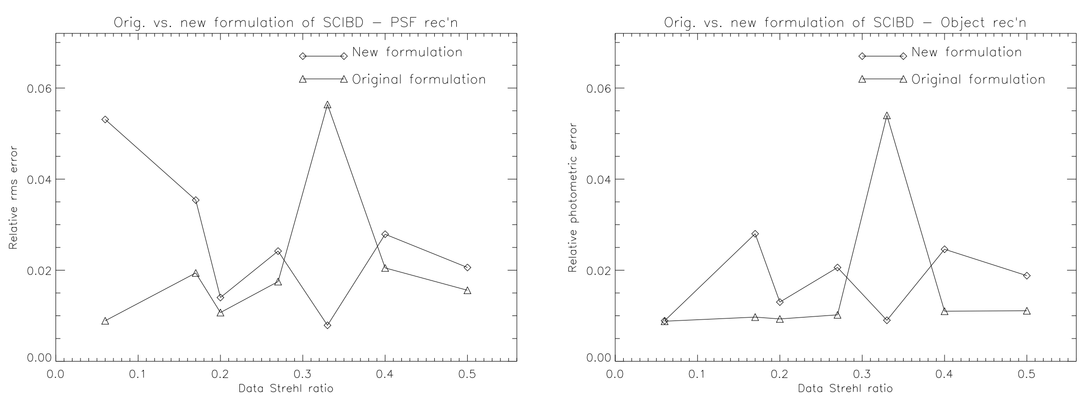

Figure 2. IBD vs. SCIBD, FLAO/LBT case, H band. Left part: relative rms error estimated on the reconstructed PSF. Right part: relative photometric error estimated on the reconstructed object.

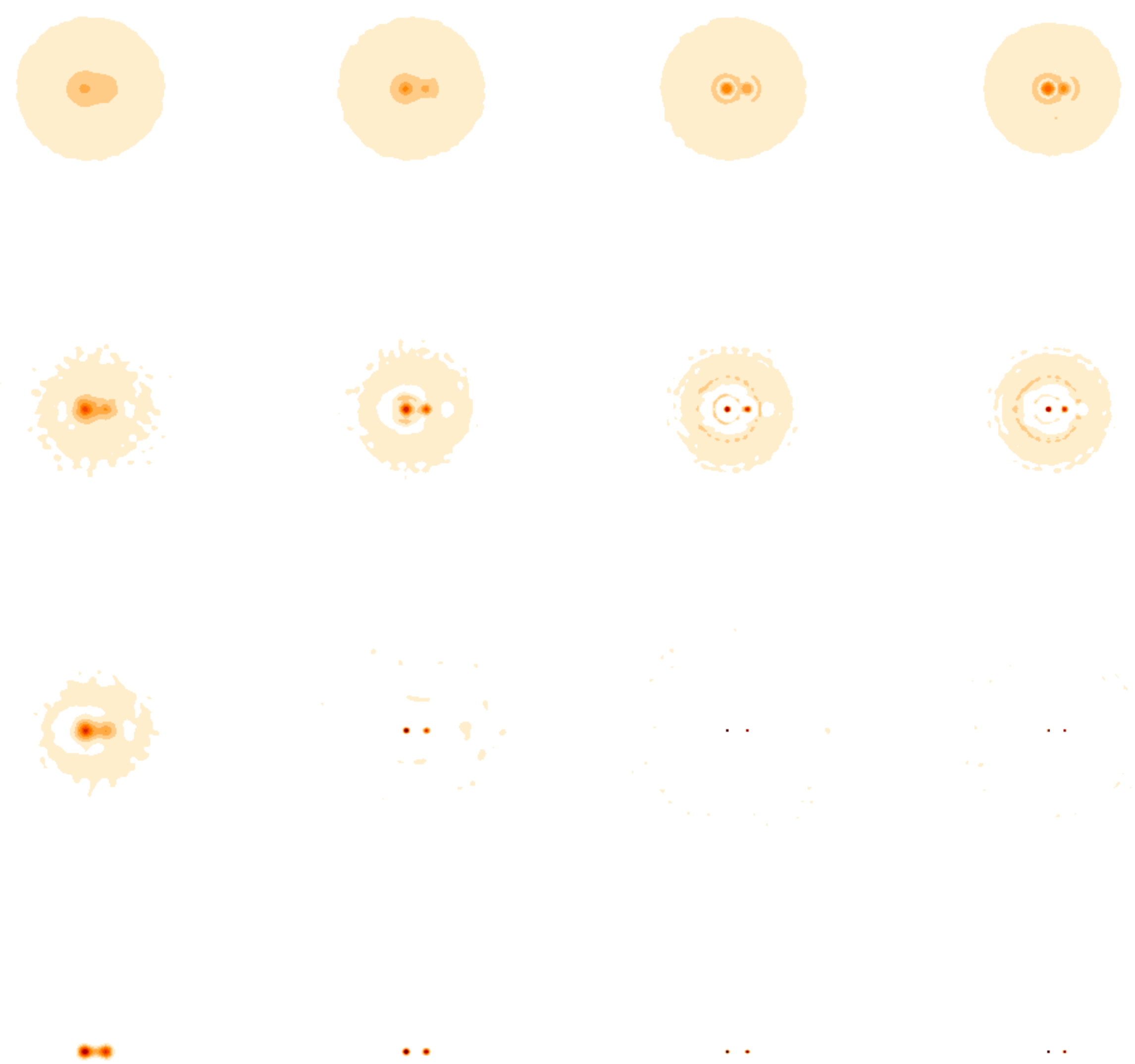

Figure 3. IBD vs. SCIBD, ODISSEE/MéO case, R band. From left to right: SR of 0.04, 0.11, 0.21, 0.31. From top to bottom: raw images, IBD reconstructions, SCIBD reconstructions, inverse-crime RL reconstructions.

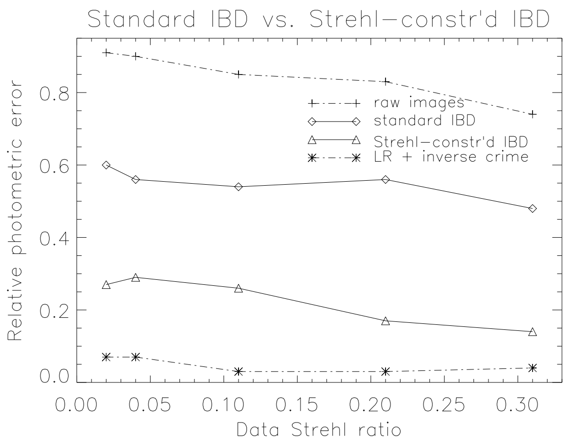

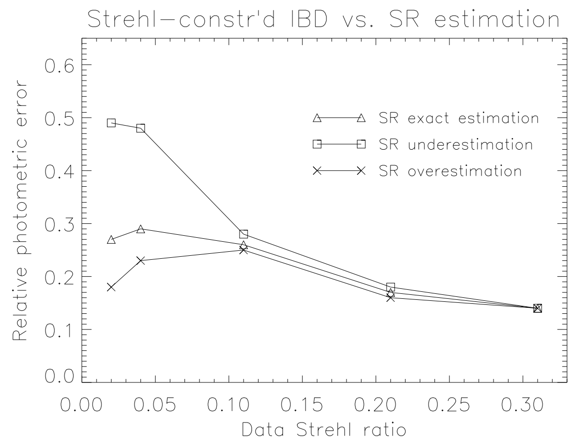

Figure 4. Left: IBD vs. SCIBD, errors. Right: SCIBD, robustness.

shows quantitatively again the gain of using the Strehl constraint in the framework of IBD. And, finally, it shows that the use of the SC permits to have results which situates at halfway from the ideal deconvolution case represented by the inverse-crime RL result.

We have then performed a study about the robustness of our SCIBD algorithm (in its original formulation) with respect to SR evaluation, considering both underestimation and overestimation of the SR as an input of the algorithm, and hence evaluating how this kind of bad estimation impacts the final reconstruction. Next table shows the values considered for both cases of bad estimation and for each actual data SR, while right part of Fig. 4 shows the result of this robustness study in a quantitative manner. It is clear from this plot that there should be a slight preference for overestimation, which tends to limit in practice the PSF blurring at the exit of the PSF box.

Data Strehl ratio	0.31	0.21	0.11	0.04	0.02
Strehl ratio overestimation considered	0.50	0.35	0.20	0.08	0.06
Strehl ratio underestimation considered	0.18	0.12	0.06	0.02	0.01

Hence we can conclude on this point that considering the SC is important in order to evitate the reconstructed PSF to diverge towards a single pixel with very high unrealistic correponding SR, but that an exagerated blurring of the reconstructed PSF does not lead to optimal results neither.

4. CONCLUSION

We have presented the last results concerning the development and study of our SCIBD method applied to post-AO partially corrected images. Its two flavors presented, both implemented within the `Software Package AIRY`, v. 6.1, are shown to give similar results on the case-study of simulated H-band FLAO/LBT-like simulated data, with SR down to 0.06. An extension towards visible wavelenghts, namely for the case-study of ODISSEE/MéO in band R (again based on simulations), confirms the gain obtained by SCIBD with respect to standard IBD. It also permits to test the robustness of our method with respect to SR estimation, showing a slight preference for overestimation rather than underestimation for the lower SR considered (down to 0.02).

Perspectives concerning this work include: (1) to apply the method to real data, and (2) to compare the results achieved with short-exposure approaches (Lucky imaging, advanced speckle techniques), in particular for very low SR.

The `Software Package AIRY`, as well as the whole `CAOS PSE`, can be freely downloaded from `http://lagrange.oca.eu/caos` and `http://www.airyproject.eu`.

REFERENCES

[1] Correia, S., Carbillet, M., Boccacci, P., Bertero, M., and Fini, L., "Restoration of interferometric images. I. The Software Package AIRY," *Astronomy and Astrophysics* **387 (2)**, 733–743 (May 2002).

[2] La Camera, A., Carbillet, M., Olivieri, C., Boccacci, P., and Bertero, M. *SPIE Proc.* **8445**, 84453E (2012).

[3] Carbillet, M., Vérinaud, C., Guarracino, M., Fini, L., Lardière, O., Le Roux, B., Puglisi, A. T., Femenía, B., Riccardi, A., Anconelli, B., Correia, S., Bertero, M., and Boccacci, P., "CAOS: a numerical simulation tool for astronomical adaptive optics (and beyond)," in [*Advancements in Adaptive Optics*], Bonaccini Calia, D., Ellerbroek, B. L., and Ragazzoni, R., eds., *Proc. SPIE* **5490 (2)**, 637–648 (Oct. 2004).

[4] Carbillet, M., Desiderà, G., Augier, E., La Camera, A., Riccardi, A., Boccaletti, A., Jolissaint, L., and Ab Kabir, D., "The CAOS problem-solving environment: recent developments," in [*Adaptive Optics Systems II*], Ellerbroek, B. L., Hart, M., Hubin, N., and Wizinowich, P. L., eds., *Proc. SPIE* **7736** (July 2010).

[5] Snyder, D. L., Hammoud, A. M., and White, R. L., "Compensation for readout noise in CCD images," *J. Opt. Soc. Am. A* **10**, 1014 (1993).

[6] Snyder, D. L., Helstrom, C. W., Lanterman, A. D., Faisal, M., and White, R. L., "Compensation for readout noise in CCD images," *J. Opt. Soc. Am. A* **12**, 272–283 (1995).

[7] Shepp, L. A. and Vardi, Y., "Maximum likelihood reconstruction for emission tomography," *IEEE Trans. Med. Imaging* **1**(2), 113–122 (1982).

[8] Bertero, M., Boccacci, P., Desiderá, G., and Vicidomini, G., "Image deblurring with Poisson data: from cells to galaxies," *Inverse Problems* **25**, 123006 (2009).

[9] Geman, S. and Geman, D., "Stochastic relaxation, Gibbs distributions, and the Bayesian restoration of images," *IEEE Trans. Pattern Anal. Mach. Intell.* **6**, 721–741 (1984).

[10] Richardson, W. H., "Bayesian-Based Iterative Method of Image Restoration," *Journal of the Optical Society of America* **62**, 55 (Jan. 1972).

[11] Lucy, L. B., "An iterative technique for the rectification of observed distributions," *Astronomical Journal* **79**, 745 (June 1974).

[12] Bertero, M. and Boccacci, P., "Image restoration methods for the Large Binocular Telescope (LBT)," *Astronomy and Astrophysics Supplement* **147**, 323–333 (Dec. 2000).

[13] Hudson, H. M. and Larkin, R. S., "Accelerated image reconstruction using ordered subsets of projection data," *IEEE Trans. Medical Imaging* **13**(4), 601–609 (1994).

[14] Biggs, D. S. C. and Andrews, M., "Asymmetric iterative blind deconvolution of multi-frame images," in [*Advanced Signal Processing Algorithms, Architectures, and Implementations VIII*], L., F. T., ed., *Proceedings of SPIE* **3461**, 328–338 (1998).

[15] Bonettini, S., Zanella, R., and Zanni, L., "A scaled gradient projection method for constrained image deblurring," *Inverse Problems* **25**, 015002 (2009).

[16] Prato, M., Cavicchioli, R., Zanni, L., Boccacci, P., and Bertero, M., "Efficient deconvolution methods for astronomical imaging: algorithms and IDL-GPU codes," *Astronomy and Astrophysics* **539**, A133 (Mar. 2012).

[17] Lantéri, H., Roche, M., and Aime, C., "Penalized maximum likelihood image restoration with positivity constraints: multiplicative algorithms," *Inverse Problems* **18**, 1397 (2002).

[18] Charbonnier, P., Blanc-Féraud, L., Aubert, G., and Barlaud, M., "Deterministic edge-preserving regularization in computed imaging," *IEEE Trans. Image Process.* **6**, 298–311 (1997).

[19] Bertero, M., Boccacci, P., La Camera, A., Olivieri, C., and Carbillet, M., "Imaging with LINC-NIRVANA, the Fizeau interferometer of the Large Binocular Telescope: state of the art and open problems," *Inverse Problems* **27**, 113011 (2011).

[20] Anconelli, B., Bertero, M., Boccacci, P., Desiderà, G., Carbillet, M., and Lantéri, H., "Deconvolution of multiple images with high dynamic range and an application to LBT LINC-NIRVANA," *Astron. Astrophys.* **460**, 349–365 (2006a).

[21] Bertero, M. and Boccacci, P., "A simple method for the reduction of boundary effects in the Richardson-Lucy approach to image deconvolution," *Astron. Astrophys.* **437**, 369–374 (2005).

[22] Anconelli, B., Bertero, M., Boccacci, P., Carbillet, M., and Lantéri, H., "Reduction of boundary effects in multiple image deconvolution with an application to LBT LINC-NIRVANA," *Astron. Astrophys.* **448**, 1217–1224 (2006b).

[23] Bertero, M., Boccacci, P., Talenti, G., Zanella, R., and Zanni, L., "A discrepancy principle for poisson data," *Inverse Problems* **26**, 10500 (2010).

[24] Bertero, M. and Boccacci, P., "Super-resolution in computational imaging," *Micron* **34**, 265–273 (2003).

[25] Anconelli, B., Bertero, M., Boccacci, P., , and Carbillet, M. *Astron. Astrophys.* **431**, 747 (2005).

[26] La Camera, A., Desiderà, G., Arcidiacono, C., Boccacci, P., and Bertero, M., "Advances in the reconstruction of LBT LINC-NIRVANA images," *Astronomy and Astrophysics* **471**, 1091–1097 (2007).

[27] Desiderà, G. and Carbillet, M., "Strehl-constrained iterative blind deconvolution for post-adaptive-optics data," *Astronomy and Astrophysics* **507**, 1759–1762 (Dec. 2009).

[28] Prato, M., La Camera, A., Bonettini, S., and Bertero, M. *Inverse Problems* **29**, 065017 (Mar. 2013).

[29] Carbillet, M., Vérinaud, C., Femenía, B., Riccardi, A., and Fini, L., "Modelling astronomical adaptive optics - I. The Software Package CAOS," *Monthly Notices of the Royal Astronomical Society* **356**, 1263–1275 (Feb. 2005).